# An Ultrafast, Ultraviolet Metal–Semiconductor–Metal Photodetector Based on AlGaN with a Response Time Below 30 ps

Y. Zhao[1] and W. R. Donaldson[1,2]

[1]Laboratory for Laser Energetics, University of Rochester
[2]Department of Electrical and Computer Engineering, University of Rochester

Aluminum–gallium–nitride (AlGaN) photodetectors have been successfully fabricated with micrometer-scale metal–semiconductor–metal (MSM) structures and tested with ultrafast UV laser pulses. The measurements were taken with single-shot oscilloscopes. Pulse-broadening effects caused by the measurement system were systematically evaluated and reduced to resolve the intrinsic response time of the detector. The best-performing devices showed a response time of below 30 ps and dark currents below 10 pA. The devices showed linear response with the bias voltage and the laser energy.

The $Al_xGa_{(1-x)}N$ (where $x$ denotes the fraction of substituted aluminum) ternary alloys are particularly interesting as UV detectors because of their high tolerance to extreme environments resulting from their thermal stability and radiation hardness.[1] The wide band gap of these materials comes with the unique feature of a tunable absorption edge. The wavelength of the band edge varies from 365 to 200 nm (Ref. 2) as the Al composition changes from 0% to 100%, which makes the device visible blind or even solar blind. One interesting application for the high-energy-density–physics and inertial confinement fusion (ICF) communities would be to detect Thomson scattering in a plasma, where the probe light must be at a frequency higher than the plasma frequency.[3] Currently UV probes at 263 nm and 210 nm are being considered for these applications but semiconducting detectors in this region of the spectrum are typically slow and inefficient.

MSM photodetectors based on AlGaN, however, have been commonly reported to have extremely long decay times and high dark currents[4,5] because of the poor material quality and high defect density. Recently, we successfully fabricated detectors on high-quality AlGaN wafers. The detectors had an ultrafast response time. To our knowledge, these are the fastest UV detectors fabricated on AlGaN thin films. To resolve the response time, the detectors were tested with single-shot, high-bandwidth oscilloscopes. This is the same configuration in which these devices would be used if they were employed in ICF experiments.

The intrinsic, n-type and p-type AlGaN wafers used to fabricate the devices were purchased from Kyma Technologies.[6] The ~330 nm-thick AlGaN thin films were grown on sapphire by metal–organic chemical vapor deposition (MOCVD). All of the wafers had an approximately 10% Al composition. A thin layer (~10 nm) of AlN was inserted between the substrate and the AlGaN. Acting as a buffer layer, the AlN thin film decreases the lattice constant mismatch between the AlGaN layer and the $Al_2O_3$ substrate, significantly reducing the density of defects and improving the quality of the materials.

The devices were designed with an interdigited finger-shaped structure. The finger width and spacing were set the same at 5 $\mu$m and the active area was $50 \times 50$ $\mu m^2$. In this work, the devices were fabricated in the Integrated Nanosystems Center (URnano) at the University of Rochester. A 120-nm-thick platinum layer was chosen for the metal contact because platinum has a high work function and has been reported to form good-quality Schottky contacts on AlGaN thin films.[7–9] A 10-nm-thick titanium layer was deposited before metallization to improve the adhesion between the platinum and semiconductor. The device fabrication involved a two-layer fabrication process and precise interlayer alignment. For some devices, the first-layer fabrication deposited a 10-nm insulating layer of $SiO_2$ within the compensation pad area (without covering the interdigited area). The purpose of the

insulation layer was to reduce the dark current leakage from the compensation pad to the AlGaN thin film. Then, for all devices, the fabrication process deposited a metal contact that covered both the compensation area and portions of the finger-shaped area.

An ORIGAMI femtosecond laser ($\lambda$ = 1053 nm with 200-fs duration) from NKT Photonics served as the main oscillator for the laser system. A single pulse from the 80-MHz pulse train was selected at a 5-Hz repetition rate by an acoustic-optic modulator and injected into an in-house–built regenerative (regen) amplifier.[10] After the regen amplifier, ~1 mJ of IR light with a FWHM of 10 ps, caused by gain-bandwidth broadening in the regen amplifier, was converted to 263 nm using nonlinear beta-barium borate crystals. The 263-nm beam with a 10-ps duration and 5-Hz repetition rate was used to test the photodetectors. We used both a 45-GHz, single-shot LeCroy oscilloscope and a 12.5-GHz Tektronix oscilloscope. When the 45-GHz oscilloscope was available, it was used in single-channel mode to access the highest digitizing rate. Otherwise, both the signal and reference signal, derived by splitting off a portion of the light and illuminating a GaAs photodiode, were acquired on the 12.5-GHz oscilloscope. The slow GaAs photodiode was used to account for fluctuations in the laser intensity. For each acquired oscilloscope trace, a portion of the trace ~100 ps wide around the peak was fitted with a Gaussian function to determine the measured FWHM, $\tau_{\text{measure}}$.

The measurement system, including the oscilloscope, cable, transmission line-mounting fixture, and the incident laser, can cause pulse broadening in the acquired signal. The FWHM that we measured is not the intrinsic response time of our MSM detector but instead is the quadrature sum of the laser pulse width, the intrinsic response of the detector, the response of the measurement system, and the broadening effect of the measurement cable, which can be expressed in the following equation:

$$\tau_{\text{measure}} = \sqrt{\tau^2_{\text{intrinsic}} + \tau^2_{\text{oscilloscope}} + \tau^2_{\text{cable}} + \tau^2_{\text{laser}} + \tau^2_{\text{circuit}}}\,. \tag{1}$$

For the LeCroy oscilloscope, $\tau_{\text{oscilloscope}}$ is 7.8 ps. The pulse width of the laser, $\tau_{\text{laser}}$, is 10 ps. To evaluate the broadening effect caused by the measurement circuit, a *SPICE* simulation[11] was carried out on the circuit we used for the testing. The circuit produced a FWHM of 16.9 ps with a 10-ps pulse impulse response. Therefore, the pulse broadening that the circuit could cause, $\tau_{\text{circuit}}$, is calculated to be 13.6 ps. The cable response $\tau_{\text{cable}}$ was measured to be 22.5 ps. The measured FWHM of the signal from the AlGaN detector, as shown in Fig. 1, is 36 ps. Based on these assumption and measurements listed above, the intrinsic response of these devices is 24 ps.

We further investigated the response behavior of the detectors under different bias voltages. We changed the bias voltage from –30 V to 30 V with a B&K Precision DC Power Supply 1635, and the detector illumination remained unchanged during the test. The peak voltages under different bias voltages are plotted in Fig. 2. Clearly the detector never reached saturation, where the peak voltage was independent of the applied bias. This is unexpected behavior and may be caused by the photogenerated carri-

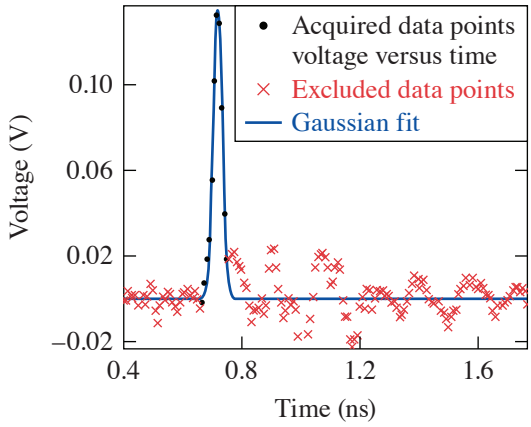


Figure 1
The response curve of the device with platinum contact fabricated on an n-type doping wafer. The finger spacing and finger width of the device are both 5 $\mu$m and the $SiO_2$ insulating layer is 10 nm thick. The signal is taken at a bias voltage of 15 V and a pulse energy of 52 nJ. The Gaussian fit is also plotted, while the other data points marked by red ×'s are excluded from the fit.

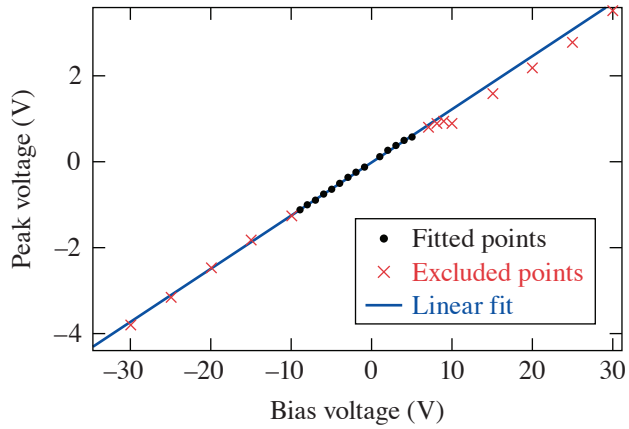


Figure 2
The peak voltage of the photodetector response under different bias voltages from –30 V to 30 V. A linear fit was made based on the data under lower biased voltage; the red ×'s points are the excluded high-voltage biased points.

ers recombining before being swept to the metal contact. As the electric field increases, the velocity of the carriers increases and more carriers reach the contact before recombining, thereby causing the peak voltage to continue to increase. Normally the peak signal is determined solely by the number of photogenerated carriers and is independent of the voltage. Since the photogenerated signal never reached the saturated regime, the responsivity could not be calculated. Further experiments are ongoing to determine the origin of the voltage dependence of the photo signal.

This material is based upon work supported by the Department of Energy National Nuclear Security Administration under Award Number DE-NA0003856, the University of Rochester, and the New York State Energy Research and Development Authority.

1. J. C. Carrano *et al*., Appl. Phys. Lett. **73**, 2405 (1998).
2. D. Walker *et al*., Appl. Phys. Lett. **74**, 762 (1999).
3. R. K. Follett *et al*., Rev. Sci. Instrum. **87**, 11E401 (2016).
4. Y. Zhao and W. R. Donaldson, J. Mater. Res. **33**, 2627 (2018).
5. Y. Zhao and W. R. Donaldson, IEEE Trans. Electron Devices **65**, 4441 (2018).
6. Kyma Technologies Inc., Raleigh, NC 27617.
7. P.-C. Chang *et al*., Thin Solid Films **498**, 133 (2006).
8. M. Brendel *et al*., Electron. Lett. **51**, 1598 (2015).
9. Y.-R. Jung *et al*., Jpn. J. Appl. Phys. **42**, 2349 (2003).
10. A. V. Okishev and J. D. Zuegel, Appl. Opt. **43**, 6180 (2004).
11. L. W. Nagel and D. O. Pederson, *SPICE (Simulation Program with Integrated Circuit Emphasis)*, EECS Department, University of California, Berkeley, Technical Report No. UCB/ERL M382 (1973).